

# Productions of heavy charged leptons via gluon fusion at LHC : A revisit

Chun Liu and Shuo Yang

*Key Laboratory of Frontiers in Theoretical Physics,  
Institute of Theoretical Physics, Chinese Academy of Sciences,  
P.O. Box 2735, Beijing 100190, China \**

## Abstract

Heavy charged lepton productions via gluon fusion at the LHC are revisited. Full loop calculations are adopted with an updated parton distribution function and electroweak data. Including contribution from new generation quarks in the loop, pair production of the sequential heavy lepton via gluon fusion at the LHC dominates over that via the Drell-Yan mechanism in some heavy lepton mass range. Exotic lepton single production of vectorlike lepton extended models is also calculated. In the later case, the gluon fusion mechanism via the Higgs exchange is emphasized. Our numerical results for both pair and single production of heavy leptons are smaller than previous studies especially for a large heavy lepton mass as a result of full loop calculation and due to the mixing angles.

PACS numbers: 14.60.Hi, 12.60.-i, 13.85.Qk

---

\*Electronic address: liuc@mail.itp.ac.cn, shuoyang@itp.ac.cn

## I. INTRODUCTION

The CERN Large Hadron Collider (LHC) is the highest energy physics experiment of our time. In addition to the Higgs particle which is the last necessity of the Standard Model (SM), its main goal is searching for the physics beyond the SM. Imaginable new physics discoveries at the LHC can be new fermions, new gauge bosons, extra Higgs and so on. Among these possibilities, we study new charged leptons. Although new lepton observation maybe challenging at the LHC, once they are produced, their decay signals are easy to be identified.

The new charged leptons are introduced in many new physics models such as grand unification theories, mirror fermions, supersymmetry and little higgs. In some models, new fermions play an important role in electroweak symmetry breaking or CP violation, and their characters may be different from the presently known fermions. Discovery of such new fermions would revolutionize our understanding of electroweak symmetry breaking and some other basic problems.

At hadron colliders, the Drell-Yan process [1] and the gluon fusion process [2] are expected to be the main mechanisms of heavy charged lepton production. In the extreme case that the new leptons are vectorlike and have no Yukawa interactions, the Drell-Yan mechanism is dominantly responsible for new lepton production. On the other hand, if the new leptons are chiral with large Yukawa couplings, their production through Higgs mediated processes can be significant, and the virtual Higgs is produced via gluon fusion. Due to the large rate of gluons at the LHC, as well as the new contributions from new quarks, the gluon fusion production can dominate over the Drell-Yan mechanism for new chiral charged leptons in some parameter region. This was also studied in refs. [3–8]. In an effort of understanding the Higgs, an extra vectorlike generation of matter is introduced within the framework of supersymmetry [9]. What is new in the lepton sector of that model after supersymmetry breaking is a vectorlike  $SU(2)_L$  singlet lepton with a mass of  $\sim \mathcal{O}(400)$  GeV. We are interested in looking at its production at the LHC. There are other vectorlike extensions to the minimal supersymmetric SM [10]. Generally, heavy leptons, even if they are vectorlike, have Yukawa interactions which may enhance their production rates. It is the gluon fusion mechanism which is the focus of this study.

In view of the current knowledge about parton distribution function, relevant electroweak

data and the top quark mass, the old results of heavy lepton production via gluon fusion should be updated. Furthermore previous studies on the gluon fusion mechanism for lepton production took tree level approximation. We will update previous studies about heavy charged lepton production via the gluon fusion mechanism in complete loop calculation. It is found that the tree level approximation should be carefully used in heavy lepton production from the gluon fusion mechanism and it is only valid in some limits.

This paper is organized as follows. In Sec. II, simple heavy fermion scenarios and their phenomenological constraints are described. In Sec. III, pair production of sequential charged fermions are calculated. Sec. IV discusses vectorlike fermion extension of the SM, and single production of the exotic fermion in this scenario. Finally, we make a discussion and give our conclusions in Sec. V.

## II. THE NEW LEPTONS

New fermions appear in various new physics models. They can be classified to be chiral or vectorlike. In this section, we will start with a description of these two scenarios of new fermions and then discuss the phenomenological bounds.

One can make a replica of a SM family to get the simplest fourth generation which is the so-called sequential fermions [11].<sup>1</sup> The sequential new leptons  $L_4$ ,  $E_4^c$  fall into the representations  $(2, -1)$ ,  $(1, 2)$  under  $SU(2)_L \otimes U(1)_Y$ , respectively.

The new leptons can also be vectorlike, where the left and right components transform the same under  $SU(2)_L \otimes U(1)_Y$ . Both vectorlike doublet leptons and vectorlike singlet leptons are simple examples [8]. The quantum numbers for vectorlike singlet lepton pair  $e_4$ ,  $e_4^c$  are  $(1, -2)$ ,  $(1, 2)$ , respectively. And those for vectorlike doublet leptons  $L_4$ ,  $L_4^c$  are  $(2, -1)$ ,  $(2, 1)$ .

Now let us consider phenomenological constraints to these scenarios. The direct experimental search of new leptons at LEP II requires that the new charged leptons should be heavier than 102 GeV and fourth neutrino heavier than 101 GeV [12]. The results for the pure Dirac neutrino and for the neutrino with a Majorana mass are slightly different. As

---

<sup>1</sup> The invisible width of Z boson and the direct search limit require that the fourth neutrino must be heavy. So a sequential fourth generation should also include a single right-handed neutrino  $\nu_{4R}$ . We will not discuss the collider phenomenology of the new neutrino in this paper.

for new quarks, the strongest bound on  $u_4$  is  $m_{u_4} > 256$  GeV [13], which comes from CDF by searching for  $u_4\bar{u}_4$  with  $u_4(\bar{u}_4)$  decay to  $W^+(W^-)$  boson and an ordinary quark. Assuming the branching ratio  $BR(d_4 \rightarrow bZ) = 1$ , CDF obtains the bound  $m_{d_4} > 268$  GeV [14]. Additionally, the constraints from the Z width require that new fermion masses are larger than  $M_Z/2$  which are weaker than those from the direct search.

For sequential fermions, the most stringent constraints are from "oblique parameters"  $S$ ,  $T$  and  $U$  [15]. These constraints can be relaxed by allowing  $T$  to vary or fourth generation masses are not degenerate [16, 17]. Recently, ref. [17] has identified a region for new sequential fermions which agrees with all experimental constraints and has minimal contributions to oblique parameters. In this paper, we will assume a similar parameter as that in [17]. Flavor physics also gives constraints on the fourth generation. Mixing parameters between the extra fermions and the ordinary three generations are subject to processes such as  $\mu \rightarrow e\gamma$  decay and  $D^0 - \bar{D}^0$  mixing. These constraints [15] are strong on the mixing between the first or second generation and the fourth generation, which suggest that mixings need to be smaller than 0.01. For the mixing between the third generation and the fourth generation, the flavor constraints are not very strong.

As for vectorlike extensions, the most important consequence is the flavor changing neutral current (FCNC). Because of introducing vectorlike fermions, there is no GIM mechanism to suppress the FCNC related to these fermions. Furthermore, there is a resultant effect on flavor diagonal neutral currents [18]. The decay width of Z boson forces this effect to be small. This constraints the mixing angles strongly. Vectorlike fermions do not contribute to "oblique parameters" in the leading order, and thus these parameters do not constrain their masses.

### III. PAIR PRODUCTION OF CHARGED SEQUENTIAL HEAVY LEPTON

Within the framework of the fourth chiral generation, pair production is the main interest about heavy charged leptons. In addition to that via the Drell-Yan process, the heavy leptons can also be produced via the gluon fusion mechanism induced by fermion loops as shown in Fig. 1. And this mechanism could dominate over the Drell-Yan mechanism in some parameter space due to the large rate of gluons at the LHC [2, 3]. There is no photon exchange diagrams, and only the Higgs and the Z boson with axial vector coupling

contributes to this gluon fusion due to Furry's theorem. As the  $ggH$  vertex in Higgs exchange diagram is a symmetric tensor while  $ggZ$  vertex in  $Z$  exchange diagram is antisymmetric, there is no interference between these two contributions. In this section, we will study the pair production of the sequential lepton via the Higgs exchange diagram and the  $Z$  exchange diagram separately.

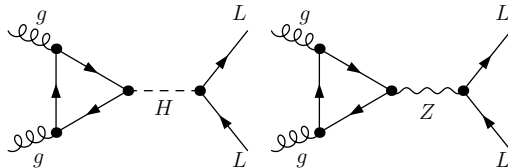


FIG. 1: Feynman diagrams for heavy lepton pair production via gluon fusion. The gluon crossing diagrams are not shown.

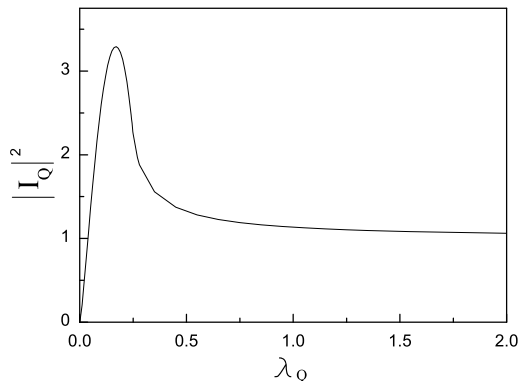


FIG. 2:  $|I_Q|^2$  as a function of  $\lambda_Q$  where  $I_Q$  is the  $ggH$  effective loop function

The Higgs exchange diagram for heavy lepton production in Fig.1 is related to Higgs production in the gluon-gluon fusion mechanism. The  $ggH$  effective Lagrangian can be presented as  $\mathcal{L} = \frac{\alpha_s}{12\pi} G^{\mu\nu} G_{\mu\nu} H I_H$  where  $I_H$  is following loop function [19],

$$I_H = \sum_Q I_Q, \quad I_Q = 3 \int_0^1 dx \int_0^{1-x} dy \frac{1 - 4xy}{1 - xy/(m_Q^2/\hat{s}) - i\epsilon}. \quad (1)$$

Replacing the C. M. energy of subprocess  $\sqrt{\hat{s}}$  by  $m_H$ , one can get the loop function for Higgs production. In general, the loop function  $I_H$  is complex and evaluation of the integral gives

$I_Q$  in terms of  $\lambda_Q = m_Q^2/\hat{s}$ ,

$$I_Q = [2\lambda_Q + \lambda_Q(4\lambda_Q - 1)f(\lambda_Q)] \quad (2)$$

where

$$f(\lambda) = \begin{cases} -2[\sin^{-1} \frac{1}{2\sqrt{\lambda}}]^2 & \text{for } \lambda > \frac{1}{4}, \\ \frac{1}{2}[\ln(\frac{1 + \sqrt{1 - 4\lambda}}{1 - \sqrt{1 - 4\lambda}}) - i\pi]^2 & \text{for } \lambda < \frac{1}{4}. \end{cases} \quad (3)$$

For convenience in discussion, we show the curve of  $|I_Q|^2$  as a function of  $\lambda_Q$  in Fig.2. <sup>2</sup> When  $m_Q$  is much heavier than  $\sqrt{\hat{s}}$ , i.e.  $\lambda_Q \gg 1$ ,  $I_Q$  reaches 1 which is just the so-called the heavy top quark limit for light Higgs production via the gluon fusion mechanism. In the small  $m_Q$  limit  $\lambda_Q \ll 1$ ,  $I_Q \rightarrow 0$ . There is also a peak for  $|I_Q|^2$  at that  $|I_Q|^2 \simeq 3.3$  for  $\lambda_Q$  being 0.17. For the process gluon-gluon fusion to a light Higgs where  $\sqrt{\hat{s}} = m_H$ , it is correct to take limit  $\lambda_Q = m_{top}^2/m_H^2 \gg 1$  for the top quark and  $\lambda_Q = m_q^2/m_H^2 \ll 1$  for light quarks. However, when it turns to heavy lepton pair production, the subprocess C.M. energy  $\sqrt{\hat{s}}$  varies from  $4m_L^2$  where  $m_L$  is the mass of the heavy lepton to several TeV, and thus the  $\lambda_Q$  is not fixed. In ref. [2], it was assumed that  $I_Q$  receives a value of unity from every quark with  $m_Q > m_L$ , which is a rough approximation. However, in some later studies  $I_Q$  was taken to be unity irrespective of the relation between  $m_Q$  and  $m_L$  and the variance of  $\sqrt{\hat{s}}$ . That is unreasonable and would overestimate the cross section for large  $m_L$ . In fact the effective function  $I_H$  should be carefully used for different  $\lambda_Q$  and it is better to calculate the cross section in loop for dilepton production from gluon fusion. We deduce the interaction vertices of ggH and ggZ and express them in terms of Passarino-Veltman scalar loop functions [21]. The cross sections are calculated in completed loop calculation with LoopTools [22]. Detailed representations are shown in appendix. We have used CTEQ6L [23] parton distribution function with factorization scale  $\mu_f = 2m_L$ . The input parameters relevant to our computation are  $m_t = 172.7$  GeV [24],  $m_b(m_b) = 4.2$  GeV,  $m_Z = 91.1876$  GeV,  $\sin^2 \theta_W = 0.2315$ ,  $\alpha_e(M_Z) = 1/128.8$  and the two-loop running coupling constant  $\alpha_s(M_Z) = 0.1176$  [15].

Fig.3 plots the cross section for new sequential lepton pair production at the LHC with  $\sqrt{s} = 14$  TeV versus the mass parameter  $m_L$  of the new charged lepton for several choices of

---

<sup>2</sup> There is a similar diagram and a detailed discussion of  $I_H$  in [20]

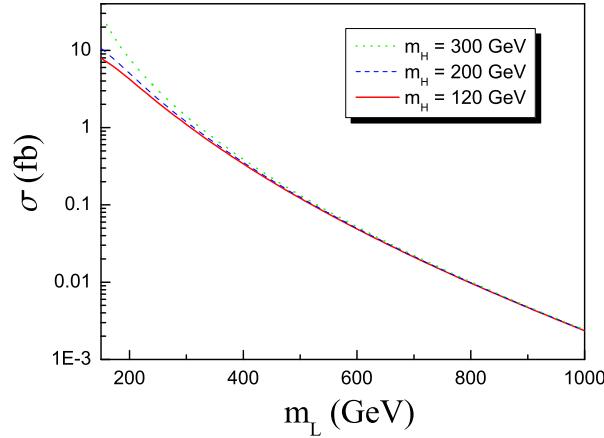


FIG. 3: Cross section for sequential heavy lepton pair production from Higgs exchange diagrams with only third generation quarks in the loops as a function of lepton mass  $m_L$  for  $m_H = 120$  GeV (solid line),  $m_H = 200$  GeV (dash line),  $m_H=300$  GeV(dot line).

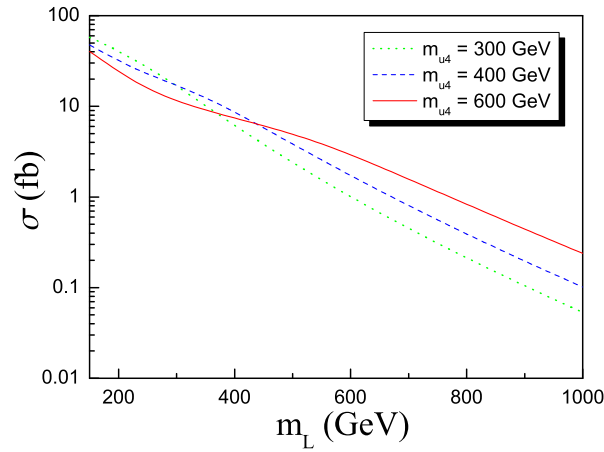


FIG. 4: Cross section for sequential heavy lepton pair production from Higgs exchange diagrams as a function of lepton mass  $m_L$  for  $m_H = 120$  GeV and  $m_{u_4} = 600$  GeV (solid line),  $m_{u_4} = 400$  GeV (dash line),  $m_{u_4}=300$  GeV (dot line).

the Higgs mass  $m_H$ . Here only contributions from the top quark and the bottom quark are included. Actually, the bottom quark's contribution is tiny in heavy lepton pair production as  $m_b/\sqrt{\hat{s}} \rightarrow 0$  for most of  $\sqrt{\hat{s}}$ , which is different from the case of Higgs production. It is found that the cross section is sensitive to the square of the mass of the new lepton. And

it can be enhanced by a heavy Higgs mass especially for a light new lepton. For a typical new lepton mass  $m_L = 200$  GeV and the Higgs mass  $m_H = 300$  GeV ( $m_H = 120$  GeV), the cross section is 7.8 fb (4.2 fb).

We also take into account the contributions from new generation sequential quarks in the loop for  $m_H = 120$  GeV, which enhances significantly the cross section in all of the parameter space as shown in Fig.4. Several typical heavy quark mass parameter values  $m_{u_4} = 300$  GeV, 400 GeV, 600 GeV and the relation  $m_{d_4} = m_{u_4} - 50$  GeV which agree well with current data [17] are used. The loop function of ggH interaction does not monotonously depend on  $\sqrt{\hat{s}}$ , the effects due to new quarks are complicated as can be seen in Fig. 4. For fixed  $m_L$  with  $m_{u_4}^2/4m_L^2 < 0.17$ , the value of  $\lambda_{u_4} = m_{u_4}^2/\hat{s}$  is smaller than 0.17 for all  $\hat{s}$  and the loop function  $I_Q$  is in the monotonous region. The heavy quark effect in this region is more important than that in the other region. It is found that the contributions from the new generation quarks are significant. For  $m_{u_4}=400$  GeV and  $m_L = 200$  GeV, the cross section is 32 fb. Even for a larger mass  $m_L = 500$  GeV, the cross section is still as large as 3.85 fb. Unlike the case of light Higgs production via gluon fusion where a generation of quarks increases the cross section by roughly a factor of 9 [17, 25], in lepton pair production the increase is smaller than 9 times in low  $m_L$  region but it is much larger than 9 times in high  $m_L$  region.

Now we consider the Z exchange diagram. The ggZ interaction vertex can be expressed as [26]:

$$F^{\alpha\mu\nu} = \sum_Q \frac{g_a g_s^2 \text{Tr}[T^a T^b]}{4\pi^2} [\varepsilon^{\mu\nu\omega\varphi} p_\omega q_\varphi k^\alpha F_1(k^2) + (\varepsilon^{\alpha\mu\omega\varphi} q^\nu - \varepsilon^{\alpha\nu\omega\varphi} q^\mu) p_\omega q_\varphi F_2(k^2) + (\varepsilon^{\alpha\mu\omega\varphi} p^\nu - \varepsilon^{\alpha\nu\omega\varphi} p^\mu) p_\omega q_\varphi F_3(k^2) + (\varepsilon^{\alpha\mu\nu\omega} (p_\omega - q_\omega))] F_4(k^2) \quad (4)$$

where  $g_a$  is the coupling of axial vector current and  $F_i(k^2)$ 's ( $i = 1-4$ ) are scalar functions,

$$F_1 = \int_0^1 dx \int_0^{1-x} dy [m_Q^2 - k^2 xy]^{-1} [(x+y)(1-x-y) + 4xy] \quad (5)$$

$$- F_2 = F_3 = \int_0^1 dx \int_0^{1-x} dy [m_Q^2 - k^2 xy]^{-1} [(x+y)(1-x-y)] \quad (6)$$

$$F_4 = 1 + \int_0^1 dx \int_0^{1-x} dy [m_Q^2 - k^2 xy]^{-1} [-2(m_Q^2 - k^2 xy) + 1/2k^2(x+y)(1-x-y)] \quad (7)$$

where the unity in  $F_4$  is the anomaly term.

Because of the different signs of axial vector coupling for up-type and down-type quarks, the contributions from up-type and down-type quarks are destructive. For the first two

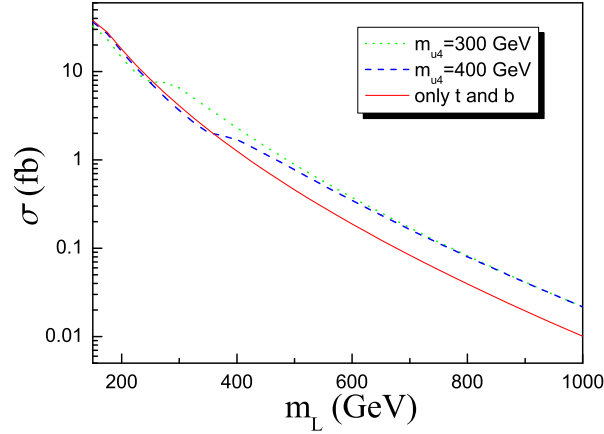


FIG. 5: Cross section for sequential heavy lepton pair production from the Z exchange diagrams as a function of lepton mass  $m_L$  for  $m_{u_4} = 300$  GeV (dot line),  $m_{u_4} = 400$  GeV (dash line) and that with the third generation quarks only (solid line).

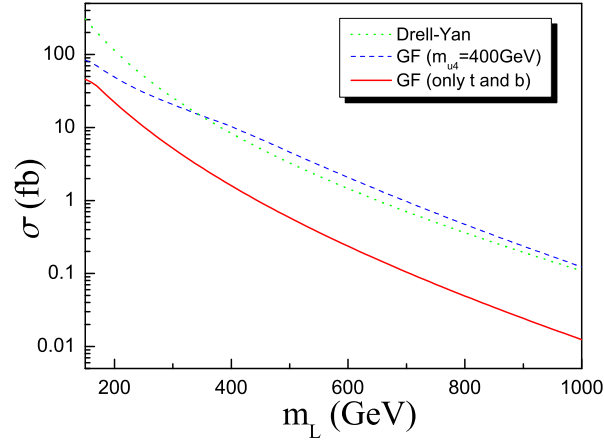


FIG. 6: Cross section for sequential heavy lepton pair production via the Drell-Yan mechanism (dot line), the gluon fusion mechanism without contribution from new quarks (solid line) and with contribution from new quarks where  $m_{u_4} = 400$  GeV,  $m_{d_4} = m_{u_4} - 50$  GeV (dash line).

generations, the mass split between up-type and down-type quarks  $\Delta m_Q \sim 0$ , so the total contribution from the first two generations is vanishing. The cross section with top quark and bottom quark contribution only is shown in the solid line in Fig. 5. The cross section with top quark and bottom quark contribution only is larger than that of the corresponding

Higgs exchange diagrams. For the heavy lepton with a mass from 250 GeV to 150 GeV, the cross section can reach 8.1 - 38 fb. We have also considered contribution from the new quarks with  $m_{u_4} = 300$  GeV or 400 GeV and  $m_{d_4} = m_{u_4} - 50$  GeV. The role of the new quarks is significant for a larger  $m_L$ . Generally, a larger split between new generation quarks will result in a higher production rate in Z exchange diagrams, which was used in previous studies, but a very large split is conflict with phenomenological constraints.

The total cross section for heavy lepton pair production via gluon fusion  $\sigma_{gg}$  is the sum of the contributions from the Z exchange diagram and the Higgs exchange diagram. In Fig. 6, this cross section is compared with that via the  $q\bar{q} \rightarrow \gamma/Z \rightarrow LL$  Drell-Yan mechanism  $\sigma_{DY}$ . If only the third generation quarks are considered,  $\sigma_{gg} < \sigma_{DY}$ . By taking into account the new generation quarks,  $\sigma_{gg}$  dominates over  $\sigma_{DY}$  in the large mass region. For instance, assuming  $m_{u_4} = 400$  GeV and  $m_{d_4} = m_{u_4} - 50$  GeV,  $\sigma_{gg} > \sigma_{DY}$  for the heavy lepton mass ranging from 350 GeV to 1000 GeV. Our numerical results about gluon fusion are smaller than previous studies[2, 3] especially for the large heavy lepton mass. This is mainly because we have used full loop calculation and due to the axial couplings.

The total cross section of heavy lepton pair production is enhanced significantly which increases the possibility of detecting the heavy lepton signal. With a luminosity  $100 \text{ fb}^{-1}$ , including contributions from new generation quarks, we predict that for the sequential lepton mass  $m_L = 250$  GeV, 8100 heavy charged lepton pair events can be produced at the LHC with  $\sqrt{s}=14$  TeV. If heavy charged lepton mass  $m_L$  is larger than heavy neutrino mass  $m_{\nu_L}$ , the main decay modes of heavy charged lepton are  $L \rightarrow \nu_L W^* \rightarrow \nu_L l \bar{\nu}_l$  and  $L \rightarrow \nu_L W^* \rightarrow \nu_L q \bar{q}'$ . In the other case  $m_L < m_N$  [27],  $L$  will only decay via Cabibbo-suppressed  $L \rightarrow \nu_\tau W^*$  with leptonic and hadronic decay of  $W^*$ .<sup>3</sup> Assuming  $m_L > m_{\nu_L}$  and the fourth generation neutrino is massless, early work [28] argued that the heavy lepton signal is buried by standard model backgrounds which mainly are single and pair production of weak bosons at the SSC with  $\sqrt{s} = 40$  TeV. However, as discussed in Sec. II, current constraints require that fourth generation neutrino holds a large mass which results in different kinematic distributions of the signal as that in ref. [28]. If considering the large contributions from new quarks and using some kinematic tricks, it is hopeful to detect the heavy lepton signal in some lower  $m_L$  region at the LHC. Further detailed studies are needed.

---

<sup>3</sup> For  $m_L < m_N$ , the most promising detecting mode of heavy lepton is  $L \bar{\nu}_L \rightarrow W^- \bar{\nu}_L \bar{\tau} W^-$ . [27]

#### IV. SINGLE PRODUCTION OF EXOTIC LEPTONS IN VECTORLIKE EXTENDED MODELS

For vectorlike fermions via the gluon fusion mechanism, both single production [5] and pair production [3, 4, 6] are possible. Because single production has a larger rate than pair production, we consider heavy lepton single production in this work. Both Drell-Yan processes [3, 5] and gluon fusion processes [5] are involved in the single production. While ref. [5] considered the Z boson mediated gluon fusion process, we also include the Higgs boson mediated gluon fusion. This can be important due to relevant large Yukawa couplings. In addition, the third generation quarks in the loop are considered. Our calculation also uses full loop calculation together with updated parton distribution function and electroweak data.

The single heavy lepton production via the gluon fusion processes is distinguishable from that via the W boson mediated Drell-Yan processes, besides the charged heavy lepton, the gluon fusion process also produces an ordinary charged lepton which can be identified experimentally in principle. Nevertheless we will compare the gluon fusion results with the Z boson mediated Drell-Yan results.

For singlet vectorlike extension, a lepton pair  $e_4$  and  $e_4^c$ , with quantum numbers  $(1, -2)$  and  $(1, 2)$  under  $SU(2)_L \otimes U(1)_Y$  are introduced. For convenience, we only consider mixing of the third generation and the new vectorlike fermion. We write down the Lagrangian relevant to lepton masses,

$$\mathcal{L} \supset y_{33} L_3 \tau_2 \Phi^* e_3^c + f e_4 e_4^c + y_{34} L_3 \tau_2 \Phi^* e_4^c + \text{h.c.}, \quad (8)$$

where  $y_{33}$  and  $y_{34}$  denote Yukawa couplings,  $\Phi$  is the Higgs doublet,  $L_3 = \begin{pmatrix} \nu_3 \\ l_3 \end{pmatrix}$  and  $e_3^c$  are the third generation lepton doublet and singlet, respectively. Note that there is no  $y_{43}$  term in the formula. After electroweak symmetry breaking  $\langle \Phi \rangle = \frac{1}{\sqrt{2}} \begin{pmatrix} 0 \\ v \end{pmatrix}$ ,

$$\mathcal{L} \supset - (l_3, e_4) \mathcal{M}^l \begin{pmatrix} e_3^c \\ e_4^c \end{pmatrix}. \quad (9)$$

The charged lepton mass matrix is given as

$$\mathcal{M}^l = \begin{pmatrix} m_{33} & m_{34} \\ 0 & f \end{pmatrix}, \quad (10)$$

where  $m_{33} = \frac{y_{33}v}{\sqrt{2}}$  and  $m_{34} = \frac{y_{34}v}{\sqrt{2}}$ . This matrix is diagonalized by two orthogonal matrices,

$$\begin{pmatrix} \cos \theta_L & -\sin \theta_L \\ \sin \theta_L & \cos \theta_L \end{pmatrix} \begin{pmatrix} m_{33} & m_{34} \\ 0 & f \end{pmatrix} \begin{pmatrix} \cos \theta_R & \sin \theta_R \\ -\sin \theta_R & \cos \theta_R \end{pmatrix} = \begin{pmatrix} m_\tau & 0 \\ 0 & m_L \end{pmatrix}, \quad (11)$$

the physical  $\tau$  lepton and the new heavy lepton  $L$  are,

$$\begin{aligned} \tau &= \cos \theta_L l_3 - \sin \theta_L e_4, & \tau^c &= \cos \theta_R e_3^c - \sin \theta_R e_4^c, \\ L &= \sin \theta_L l_3 + \cos \theta_L e_4, & L^c &= \sin \theta_R e_3^c + \cos \theta_R e_4^c. \end{aligned} \quad (12)$$

The corresponding masses and mixing parameters are

$$\begin{aligned} m_\tau^2 &= \frac{1}{2} \left( f^2 + m_{33}^2 + m_{34}^2 - \sqrt{(f^2 - m_{34}^2 - m_{33}^2)^2 + 4m_{34}^2 f^2} \right) \simeq m_{33}^2, \\ m_L^2 &= \frac{1}{2} \left( f^2 + m_{33}^2 + m_{34}^2 + \sqrt{(f^2 - m_{34}^2 - m_{33}^2)^2 + 4m_{34}^2 f^2} \right) \simeq f^2 + m_{34}^2; \\ \sin \theta_L &= \frac{1}{\sqrt{2}} \sqrt{1 - \frac{f^2 - m_{34}^2 - m_{33}^2}{\sqrt{(f^2 - m_{34}^2 - m_{33}^2)^2 + 4m_{34}^2 f^2}}} \simeq \frac{m_{34}}{f}, \\ \sin \theta_R &= \frac{1}{\sqrt{2}} \sqrt{1 - \frac{f^2 + m_{34}^2 - m_{33}^2}{\sqrt{(f^2 + m_{34}^2 - m_{33}^2)^2 + 4m_{34}^2 m_{33}^2}}} \simeq \frac{m_{33} m_{34}}{f^2}. \end{aligned} \quad (13)$$

Taking  $f > m_{34}, m_{33}$ , we have made an expansion to order of  $v/f$  and keep only leading non-vanishing results.

Now let us turn to the doublet vectorlike fermions. The vectorlike doublet extension introduces a doublet lepton pair  $L_4$  and  $L_4^c$  with quantum numbers  $(2, -1)$  and  $(2, 1)$  under  $SU(2)_L \otimes U(1)_Y$ . The Lagrangian relevant to the mass is:

$$\mathcal{L} \supset y_{33} L_3 \tau_2 \Phi^* e_3^c + f L_4 L_4^c + y_{43} L_4 \tau_2 \Phi^* e_3^c + \text{h.c.} \quad (14)$$

As in the case of the vectorlike singlet model, the masses and mixing parameters are obtained,

$$\begin{aligned}
m_\tau^2 &= \frac{1}{2} \left( f^2 + m_{33}^2 + m_{43}^2 - \sqrt{(f^2 + m_{43}^2 - m_{33}^2)^2 + 4m_{43}^2 f^2} \right) \simeq m_{33}^2, \\
m_L^2 &= \frac{1}{2} \left( f^2 + m_{33}^2 + m_{43}^2 + \sqrt{(f^2 + m_{43}^2 - m_{33}^2)^2 + 4m_{43}^2 f^2} \right) \simeq f^2 + m_{43}^2; \\
\sin \theta_L &= \frac{1}{\sqrt{2}} \sqrt{1 - \frac{f^2 + m_{43}^2 - m_{33}^2}{\sqrt{(f^2 + m_{43}^2 - m_{33}^2)^2 + 4m_{43}^2 m_{33}^2}}} \simeq \frac{m_{43} m_{33}}{f^2}, \\
\sin \theta_R &= \frac{1}{\sqrt{2}} \sqrt{1 - \frac{f^2 - m_{43}^2 - m_{33}^2}{\sqrt{(f^2 - m_{43}^2 - m_{33}^2)^2 + 4m_{43}^2 f^2}}} \simeq \frac{m_{43}}{f}.
\end{aligned} \tag{15}$$

The interaction vertices are obtained after replacing the weak eigenstates by the physical states. Higgs-fermion-fermion and Z-fermion-fermion interactions for physical  $\tau$  and  $L$  are listed in Table I. The feynman rules for  $ZLL$   $ZL\tau$  agree with that given in ref. [29]. The  $L$  related tree level FCNC is explicitly seen.

	Vectorlike singlet model	Vectorlike doublet model
$H\bar{\tau}\tau$	$\frac{m_\tau c_L c_R}{v}$	$\frac{m_\tau c_L c_R}{v}$
$H\bar{L}L$	$\frac{y_{34}}{\sqrt{2}} s_L c_R$	$\frac{y_{43}}{\sqrt{2}} s_R c_L$
$H\bar{L}\tau$	$\frac{y_{33}}{\sqrt{2}} s_L c_R P_R + \frac{y_{34}}{\sqrt{2}} c_L c_R P_L$	$\frac{y_{33}}{\sqrt{2}} s_L c_R P_R + \frac{y_{43}}{\sqrt{2}} c_L c_R P_R$
$Z\bar{\tau}\tau$	$-\frac{g}{2 \cos \theta_W} \gamma_\mu (2 \sin^2 \theta_W - P_L c_L^2)$	$-\frac{g}{2 \cos \theta_W} \gamma_\mu \left( 2 \sin^2 \theta_W - \frac{1}{2} (1 + s_R^2) + \frac{1}{2} c_R^2 \gamma_5 \right)$
$Z\bar{L}L$	$-\frac{g}{2 \cos \theta_W} \gamma_\mu (2 \sin^2 \theta_W - P_L s_L^2)$	$-\frac{g}{2 \cos \theta_W} \gamma_\mu \left( 2 \sin^2 \theta_W - \frac{1}{2} (1 + c_R^2) + \frac{1}{2} s_R^2 \gamma_5 \right)$
$Z\bar{L}\tau$	$\frac{g}{2 \cos \theta_W} \gamma_\mu (P_L c_L s_L)$	$-\frac{g}{2 \cos \theta_W} \gamma_\mu (P_R c_R s_R)$

TABLE I: Higgs-fermion-fermion and Z-fermion-fermion interactions in the vectorlike singlet model and the vectorlike doublet model.  $P_{L,R} = \frac{1 \mp \gamma_5}{2}$ ,  $s = \sin \theta$ ,  $c = \cos \theta$ .

The main phenomenological constraints come from the branching ratio of  $Z \rightarrow \tau\tau$ . Non-vanishing  $\sin \theta_L$  results in that  $Z \rightarrow \tau\tau$  deviates from SM prediction. The current experimental data and SM prediction are [15]

$$\begin{aligned}
\Gamma^{\text{exp}}(Z \rightarrow \tau\tau) &= (84.09 \pm 0.2) \text{ MeV}, \\
\Gamma^{\text{SM}}(Z \rightarrow \tau\tau) &= (83.82 \pm 0.1) \text{ MeV}.
\end{aligned} \tag{16}$$

Considering the central value difference and  $3\sigma$  uncertainties of both experimental and theoretical results, the  $Z \rightarrow \tau\tau$  decay width still allows its one percent at most coming from new physics (which corresponds to  $\sim 0.3\%$  of the branching ratio). Requiring the uncertainty of the  $Z \rightarrow \tau\tau$  width being smaller than 1%, we get  $\sin\theta_L < 0.0686$  in the vectorlike singlet case.

New interactions  $Z\bar{L}\tau$  and  $H\bar{L}\tau$  provide the mechanism for single production of exotic leptons via gluon fusion. We perform calculation with LoopTools [22]. The results of the cross section are shown in Fig. 7 by taking  $\sin\theta_L = 0.05$ . They include both  $\bar{\tau}L$  and  $\tau\bar{L}$  production. The figure also shows that of the Z boson mediated Drell-Yan process for comparison. We see that Drell-Yan always dominates over gluon fusion. For  $m_L = 150 - 250$  GeV, the cross section via gluon fusion is about 0.3 fb while that via Drell-Yan is several fb which is marginally within the detect ability at the LHC. For  $m_L > 250$  GeV, even the Drell-Yan cross section is smaller than 1 fb, this is small for such heavy lepton detection.

One way to enhance the gluon fusion mechanism is to consider an additional generation of sequential fermions with large Yukawa couplings. Namely the physics is the SM plus a fourth chiral generation and the vectorlike singlet charged lepton. New sequential quark loops with  $m_U = 400$  GeV and  $m_D = m_U - 40$  GeV, for an example, increase gluon fusion contribution in single production processes. Then the cross sections of Higgs mediated gluon fusion are larger than those of Z boson mediated gluon fusion. And the gluon fusion mechanism can dominate over the Drell-Yan mechanism, as shown in Fig. 7 for  $m_L > 350$  GeV. In this case the cross section can be as large as 0.3 fb. This again is still challengingly small for its detection at the LHC.

Let us make few remarks. (1) Compared to heavy sequential lepton pair production studied in the last section, the vectorlike lepton single production rate is small, in spite of the phase space enhancement. This is mainly due to that we have used full loop calculation. The smallness is also due to suppression of  $\sin\theta_L$  which is strongly constrained by the branching ratio of  $Z \rightarrow \tau\tau$ . Note that we have used  $\sin\theta_L$  being 0.05 which is just half of that adopted in previous studies [5]. (2) For vectorlike lepton pair production, because  $HLL$  interaction and axial vector current  $ZLL$  interaction are proportional to  $\sin\theta_L$  and  $\sin\theta_L^2$ , respectively, in this model, the cross sections of the Higgs exchange diagram and the Z exchange diagram are suppressed significantly by  $\sin\theta_L$  in certain power. (3) The phenomenology analysis for vectorlike doublet lepton models is similar to the singlet case.

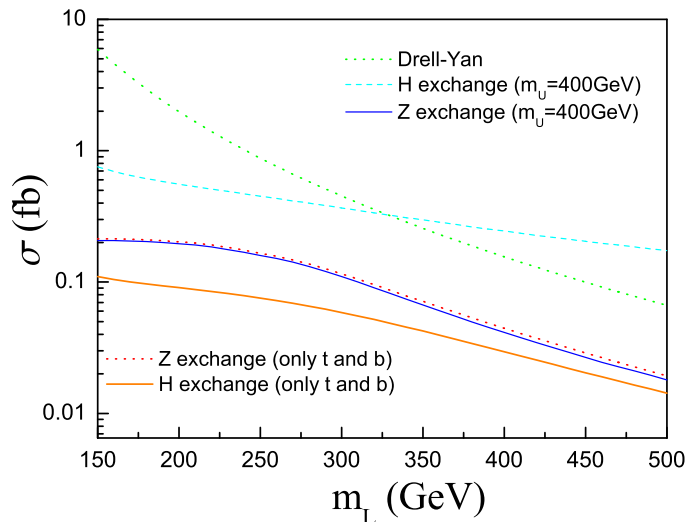


FIG. 7: Cross sections for vectorlike singlet lepton single production via the gluon fusion mechanism: Higgs exchange (lower solid line) and Z exchange (lower dot line) without new sequential fermions; and Higgs exchange (dash line) and Z exchange (upper solid line) with additional sequential fermions where  $m_U = 400$  GeV,  $m_D = m_U - 50$  GeV. The Drell-Yan mechanism (upper dot line) is given for comparison.

The production results are similar to the above singlet scenario. So we will not discuss the doublet lepton scenario further.

## V. CONCLUSION

In this paper we have revisited heavy lepton productions at the LHC. Our focus is the gluon fusion mechanism which can be important due to large rate of gluons at the LHC. If contribution from new generation quarks is considered, the cross sections via the gluon fusion mechanism can be enhanced significantly. The pair production of new sequential heavy leptons from gluon fusion at the LHC dominates over that of the Drell-Yan mechanism in the large lepton mass region. With a luminosity of  $100 \text{ fb}^{-1}$ , we predict that for the sequential lepton mass  $m_L = 250$  GeV, 8100 heavy charged lepton pair events can be produced at the LHC with  $\sqrt{s} = 14$  TeV.

We have also calculated exotic lepton single production in vectorlike lepton extended

models. In the gluon fusion mechanism, we have included the Higgs exchange. However, the production rate for exotic lepton is small due to suppression of the mixing parameter. Our numerical results for both pair and single production of heavy leptons are smaller than previous studies especially for the heavy lepton in the large mass region. The main reason is that we have not used tree level approximation. In the loop computation, we have also adopted updated parton distribution function and new electroweak physics data.

## Acknowledgments

The authors would like to thank Tao Han, Zong-guo Si, Wen-Long Sang and Lei Wang for helpful discussions. This work was supported in part by the National Science Foundation of China under Grant Nos. 90503002 and 10821504, and by the National Basic Research Program of China under Grant No. 2010CB833000.

## Appendix

The cross section for the 2-2 process at hadron colliders is

$$\sigma(P_A P_B \rightarrow F_3 F_4) = \sum_{a,b} \int dx_1 dx_2 f_{a/A}(x_1, Q^2) f_{b/B}(x_2, Q^2) \frac{P_{out}}{32\pi^2 \hat{s}^{3/2}} |\overline{\mathcal{M}}|^2 d\Omega, \quad (\text{A.1})$$

where  $P_{out} = \sqrt{\frac{(\hat{s} + m_4^2 - m_3^2)^2}{4\hat{s}} - m_4^2}$ , and  $m_3$  and  $m_4$  are the masses of final states  $F_3$  and  $F_4$ , respectively. For the Higgs and Z exchange diagrams of the pair production and single production of heavy leptons, the Feynman amplitudes are represented as follows.

$$\mathcal{M}_H = \frac{g_s^2}{4\pi^2 v} I_H (g^{\mu\nu} - \frac{2p_1^\mu p_2^\nu}{\hat{s}}) \epsilon_\mu(p_1) \epsilon_\nu(p_2) \frac{i}{\hat{s} - m_H^2 + iM_H \Gamma_H} \frac{m_L}{v} \bar{u}(p_3) v(p_4). \quad (\text{A.2})$$

$$\mathcal{M}_Z = F^{\alpha\mu\nu} \epsilon_\mu(p_1) \epsilon_\nu(p_2) \frac{i(-g_{\alpha\beta} + k_\alpha k_\beta / m_Z^2)}{\hat{s} - m_Z^2 + iM_Z \Gamma_Z} \bar{u}(p_3) i\gamma_\beta (g_v + g_a \gamma_5) v(p_4). \quad (\text{A.3})$$

In formula (A.3),  $F^{\alpha\mu\nu}$  is the ggZ interaction vertex as represented in formula (5). The  $I_H$  represented in Passarino-Veltman is:

$$I_H = \sum_Q m_Q^2 \left[ \left(1 + (2m_Q^2 - \frac{\hat{s}}{2}) C0[0, 0, \hat{s}, m_Q^2, m_Q^2, m_Q^2]\right) \right], \quad (\text{A.4})$$

and  $F'_i$ s in  $F^{\alpha\mu\nu}$  represented in scalar loop functions are:

$$F_1 = -\frac{1}{\hat{s}}(B0[0, m_Q^2, m_Q^2] - B0[\hat{s}, m_Q^2, m_Q^2] + 1 + 2C0[0, 0, \hat{s}, m_Q^2, m_Q^2, m_Q^2]m_Q^2), \quad (\text{A.5})$$

$$-F_2 = F_3 = \frac{2}{\hat{s}} \left[ -\frac{1}{2}(B0[0, m_Q^2, m_Q^2] - B0[\hat{s}, m_Q^2, m_Q^2] + 1 - 2C0[0, 0, \hat{s}, m_Q^2, m_Q^2, m_Q^2]m_Q^2) + 1 \right], \quad (\text{A.6})$$

$$F_4 = -\frac{1}{2}(B0[0, m_Q^2, m_Q^2] - B0[\hat{s}, m_Q^2, m_Q^2] + 1 - 2C0[0, 0, \hat{s}, m_Q^2, m_Q^2, m_Q^2]m_Q^2) + 1, \quad (\text{A.7})$$

and LoopTools [22] is used for the numerical calculation of the scalar loop functions.

The general representations of Passarino-Veltman scalar loop functions  $B0$  and  $C0$  are [21]:

$$B0[p_1^2, m_1^2, m_2^2] = \frac{1}{i\pi^2} \int d^D q \frac{1}{[q^2 - m_1^2][(q + p_1)^2 - m_2^2]}. \quad (\text{A.8})$$

$$C0[p_1^2, p_2^2, (p_1 + p_2)^2, m_1^2, m_2^2, m_3^2] = \frac{1}{i\pi^2} \int d^D q \frac{1}{[q^2 - m_1^2][(q + p_1)^2 - m_2^2][(q + p_1 + p_2)^2 - m_3^2]}. \quad (\text{A.9})$$

- 
- [1] S.D. Drell and T.-M. Yan, Phys. Rev. Lett. **25**, 316 (1970).
  - [2] S.S.D. Willenbrock and D.A. Dicus, Phys. Lett. B **156**, 429 (1985).
  - [3] P.H. Frampton, D. Ng, M. Sher and Y. Yuan, Phys. Rev. D **48**, 3128 (1993).
  - [4] J.E. Cieza Montalvo, O.J.P. Éboli and S.F. Novaes, Phys. Rev. D **46**, 181 (1992); V. Barger and W.-Y. Keung, Phys. Rev. D **34**, 2902 (1986); M.M. Boyce, M.A. Doncheski and H. König, Phys. Rev. D **55**, 68 (1997).
  - [5] Y.A. Coutinho, J.A. Martins Simões, C.M. Porto and P.P. Queiroz Filho, Phys. Rev. D **57**, 6975 (1998).
  - [6] J.E. Cieza Montalvo and P.P. de Queiroz Filho Phys. Rev. D **66**, 055003 (2002).
  - [7] I. Caprini and M. Rotaru, Mod. Phys. Lett. A **21**, 1999 (2006).
  - [8] For a review, see P.H. Frampton, P.Q. Hung and M. Sher, Phys. Rep. **330**, 263 (2000).
  - [9] C. Liu, Phys. Rev. D **80**, 035004 (2009).
  - [10] V. Barger, J. Jiang, P. Langacker and T.-J. Li, Int. J. Mod. Phys. A **22**, 6203 (2007); K.S. Babu, I. Gogoladze, M.U. Rehman and Q. Shafi, Phys. Rev. D **78**, 055017 (2008); T. Ibrahim and P. Nath, Phys. Rev. D **78**, 075013 (2008); S.P. Martin, Phys. Rev. D **81**, 035004 (2010); P.W. Graham, A. Ismail, S. Rajendran and P. Saraswat, arXiv:0910.3020.

- [11] For a recent review, see B. Holdom, W.S. Hou, T. Hurth, M.L. Mangano, S. Sultansoy and G. Unel, *PMC Phys.* **A3**, 4 (2009).
- [12] P. Achard *et al.*(L3 Collaboration), *Phys. Lett. B* **517**,75 (2001); G. Abbiendi *et al.*(OPAL Collaboration), *Phys. Lett. B* **572**, 8 (2003).
- [13] T. Aaltonen *et al.*(CDF Collaboration), *Phys. Rev. Lett.* **100**, 161803 (2008).
- [14] T. Aaltonen *et al.*(CDF Collaboration), *Phys. Rev. D* **76**, 072006 (2007).
- [15] C. Amsler *et al.*(Particle Data Group), *Phys. Lett. B* **667**, 1 (2008).
- [16] M. Maltoni, V.A. Novikov, L.B. Okun, A.N. Rozanov and M.I. Vysotsky, *Phys. Lett. B* **476**, 107 (2000); H.-J. He, N. Polonsky and S.-f. Su, *Phys. Rev. D* **64**, 053004 (2001); B. Holdom, *Phys. Rev. D* **54**, R721 (1996); M. Bobrowski, A. Lenz, J. Riedl, and J. Rohrwild, *Phys. Rev. D* **79**, 113006 (2009).
- [17] G.D. Kribs, T. Plehn, M. Spannowsky and T.M.P. Tait, *Phys. Rev. D* **76**, 075016 (2007).
- [18] V. Barger, M. S. Berger, R. J. N. Phillips, *Phys. Rev. D* **52**, 1663 (1995).
- [19] H. M. Georgi, S. L. Glashow, M. E. Machacek, and D. V. Nanopoulos, *Phys. Rev. Lett.* **40**, 692 (1978).
- [20] V. Barger and R. Philips, *Collider Physics*, (Addison-Wesley Publishing Company, Redwood City, 1988).
- [21] G. Passarino and M. Veltman, *Nucl. Phys. B* **160**, 151 (1979); G. 't Hooft and M. Veltman, *Nucl. Phys. B* **153**, 365 (1979).
- [22] T. Hahn and M. Perez-Victoria, *Comput. Phys. Commun.* **118**, 153 (1999)
- [23] J. Pumplin *et al.*, (CTEQ Collaboration), *JHEP* **02**, 032 (2006).
- [24] Tevatron Electroweak Working Group, For the CDF and DØ Collaborations, hep-ex/0703034.
- [25] N.B. Schmidt, S.A. Cetin, S. Istin and S. Sultansoy, arXiv:0908.2653.
- [26] J.S. Bell and R. Jackiw, *Nuovo Cim. A* **60**, 47 (1969).
- [27] W.S. Hou and G.G. Wong, *Phys. Rev. D* **49**, 3643 (1994).
- [28] V. Barger, T. Han, J. Ohnemus, *Phys. Rev. D* **37**, 1174 (1988).
- [29] J.E. Cieza Montalvo, *Phys. Rev. D* **59**, 095007 (1999).